Process Safety and Environmental Protection 188 (2024) 664–676

Contents lists available at ScienceDirect

Process Safety and Environmental Protection

journal homepage: www.journals.elsevier.com/process-safety-and-environmental-protection

Performance assessment of Brayton-biogas multigeneration system fed by the municipal wastes

Damla Kılıç Erikgenoğlu [1,*], Oğuz Arslan [2]

Bilecik Şeyh Edebali University, Faculty of Engineering, Department of Mechanical Engineering, Bilecik, Turkey

ARTICLE INFO

Keywords:
Biogas combustion
Brayton cycle
Multigeneration system
Municipal waste
Waste heat

ABSTRACT

Increasing energy demands require evaluating all kinds of sources, such as biomass. Municipal waste was assessed as the primary biomass source in a two-stage digester tank system for effective biogas production. The produced biogas was later evaluated in a cogeneration system, including a Brayton power cycle and heating circuit for the residential and domestic hot water. Also, the generated heat was used to provide the necessary heat in the digester tanks for the available environmental biogas production conditions. The proposed system was thermodynamically evaluated through energy and exergy analysis. In this context, the energy and exergy efficiencies of the system were determined as 43.40 % and 41.25 %, respectively. The net power production of the system was determined as 876.83 kW. Thanks to waste heat energy, 1136 residences can be provided with hot water in summer, and 565 residences can be supplied with hot water and heating in winter.

1. Introduction

The worldwide energy demand is consistently increasing, depending on industrial developments, urbanisation, and technological advancements. Fossil fuels, which are traditional energy sources, still significantly meet a substantial portion of global energy needs. However, the limited nature of these resources and their contribution to carbon emissions associated with climate change have accelerated research and investments in renewable energy sources. Among the prominent alternative energy sources, biomass has emerged as an increasingly important source in recent years. Biomass energy is derived from various organic wastes, such as animal manure and municipal and agricultural waste (Benato and Macor, 2017). Biogas formed by the fermentation of these wastes consists of methane and carbon dioxide and a few amounts of gases such as hydrogen sulfide, nitrogen oxide, oxygen, ammonia and water vapor (Mahmoodi-Eshkaftaki and Ebrahimi, 2019; Seirafi, 2024). Using these gases, which have a greenhouse gas effect, in the biogas facility enables effective waste management and reduction of harmful gas emissions (Kour et al., 2024). While biogas increases environmental sustainability by integrating waste management and energy production, it also plays a vital role in combating climate change emissions (Barua and Kalamdhad, 2019; Zhang et al., 2023a,2023b). Therefore, establishing and disseminating biogas facilities is considered an essential strategy in terms of both environmental and energy.

In recent years, efforts to recover waste heat released into the atmosphere and increase system performance have gained importance. In this context, biogas-driven cogeneration systems attract attention. There are many studies on this subject in the literature. Gholizadeh et al. (2019) studied the electricity/cooling cogeneration system combined with a biogas-powered gas turbine cycle from a thermodynamic and economic perspective. The energy and exergy efficiencies of the combined system were obtained as 67.33 % and 19.15 %. Zhang et al. (2023) investigated the impact of the biogas-driven cogeneration cycle on carbon emission reduction. It was reported that 496.86 million tons of CO_2 emissions could be reduced when the proposed system was used. Anvari et al. (2023) examined different types of steam injection to improve the performance of a biogas-fired cogeneration cycle. As a result, it was stated that injecting steam into the combustion chamber (CC) and gasifier increased system performance. Bai et al. (2023) investigated a cogeneration system that utilises geothermal and biomass energy. The plant's exergy efficiency, unit product cost, and CO_2 emissions were found to be 44.12 %, 66.97 $/MWh, and 0.7105 kg/kWh, respectively. The results demonstrate the feasibility of the hybrid system. Zare et al. (2019) operated a cogeneration cycle that produced 30 MW of electricity using biogas and natural gas. The system consists of

* Corresponding author.
E-mail addresses: damla.kilic@bilecik.edu.tr (D.K. Erikgenoğlu), oguz.arslan@bilecik.edu.tr (O. Arslan).
[1] ORCID: 0000-0001-8728-1068
[2] ORCID: 0000-0001-8233-831X

https://doi.org/10.1016/j.psep.2024.05.097
Received 12 February 2024; Received in revised form 16 May 2024; Accepted 22 May 2024
Available online 23 May 2024
0957-5820/© 2024 Institution of Chemical Engineers. Published by Elsevier Ltd. All rights are reserved, including those for text and data mining, AI training, and similar technologies.

Nomenclature

A	area (m2)
C_{CH_4}	methane content (%)
c_p	specific heat (kJ/kg·C)
D	diameter (m)
DM	dry matter
$\dot{E}$	energy rate (kW)
$\dot{E}x$	exergy rate (kW)
H	height (m)
h	convection coefficient (W/m^2·K), enthalpy (kJ/kg)
$\overline{h}$	molar enthalpy (kJ/kmole)
I	exergy destruction rate (kW)
k	conductivity coefficient (W/m·K)
$\dot{m}$	mass flow (kg/s)
m_m	waste amount (tons/day)
$\dot{n}$	mole ratio (kmole/s)
P	pressure (kPa)
r_{cr}	critical radius (m)
$\dot{Q}$	heat rate (kW)
RH	residence heating
R_u	universal gas constant (kJ/kmole·K)
s	entropy (kJ/kg.K)
T	temperature °C
U	heat transfer coefficient (W/m^2·K)
V_{bio}	biogas production (m^3/day)
V_{CH_4}	methane gas amount
V_D	digester tank volüme (m^3)
$\dot{W}$	power (kW)
y_i	molar fraction

Greek letter

α_{th}	stoichiometric coefficient
ε	exergy efficieny (%)
η	energy efficiency (%)
λ	excess air coefficient
μ_{bio}	biogas yield
ρ	density (kg/m^3)

Subscript

0	dead state
a	ambient
ch	chemical
d	destruction
f	fuel
i	inlet
m	manure
M	mixer
o	outlet
ph	physical
$prod$	product

Abbreviations

AC	air compressor
CC	combustion chamber
CR	compression rate
DM	dry matter
DHW	domestic hot water
GT	gas turbine
HE	heat exchanger
HRT	hydraulic retention time
LHV	lower heating value
ODM	organic dry matter
P	pump
RH	residence heating
TES	thermal energy storage

an anaerobic digester, a steam generator, and a heat exchanger (HE). When the system was compared for the blend of natural gas and biogas, the exergy efficiency was determined as 50.5 % with a product cost of 3665 $/h. They calculated that the proposed system could produce 1368 kW of electricity. They also reported that the system had an exergy efficiency of 38.91 % with a power generation rate of 1 GJ. Seirafi et al. (2024) conducted a thermodynamic analysis of the power-hydrogen cogeneration unit fueled by biogas. The combustion of biogas was reported to increase the system efficiency by 74 %. Cao et al. (2021) examined the biogas-powered cogeneration cycle for both summer and winter. They stated that the system efficiency is higher during winter than in summer. Accordingly, energy efficiency in summer and winter is 79.2 % and 70.70 %, respectively. Campero et al. (2023) optimised a cogeneration cycle based on the Brayton-Stirling cycle fueled by biogas. The results show that the system efficiency reaches 85 % when the turbine inlet temperature is 1273 K, the pressure ratio is 0.4, and the dead volume of the Stirling engine is 0.3. Holik et al. (2021) investigated waste heat utilisation from the cogeneration cycle fueled by biogas in the Rankine cycle. The system efficiency was stated as 66.7 %. The study's findings suggest that the waste heat recovery system employing the Rankine cycle proves to be more cost-effective than the system utilising the organic Rankine cycle with toluene as the working fluid.

Biogas energy is also widely used in multigeneration systems. Su et al. (2020) proposed a biogas-powered combined heat and power system based on a gas turbine cycle. By operating the system, less natural gas consumption occurred, and significant waste heat recycling was achieved. Huang et al. (2024) examined the reuse of a part of the heat obtained from the combined power cycle in the biogas process. The results revealed that the thermal and exergy efficiency of the system increased by 28.39 % and 8.31 %. Lin et al. (2023) examined a multigeneration system in which biogas obtained from sewage sludge and solar energy were integrated. As a result, it was stated that the system could produce 18.1 MW of power and significantly reduce CO_2 emissions. Zhou et al. (2023) analysed a system consisting of two-stage combined cooling and power cycles operated with biogas. As a result of the optimisation, the energy and exergy efficiencies of the system were determined to be 80.4 % and 41.24 %, respectively. Additionally, it was determined that 424.1 kW of cooling and 1.864 kW of electricity could be generated from the cycle. Jabari et al. (2022) designed a combined freshwater and power generation network. Biogas contributes to power production by supporting a gas turbine by using it instead of natural gas. The system produced 5.8 MW of electricity with an efficiency of 37 % and 168 litres of water per minute. Zhao et al. (2024) investigated the use of flue gas obtained from industrial silicon production and biogas in power plants. To increase the proposed system's efficiency, waste heat in the subcycles was examined. The results showed that utilising waste heat resulted in a significant increase in system efficiency.

The literature shows that biogas energy is an alternative tool to evaluate the wastes for energy generation. In this study, a cogeneration system was designed and analysed to evaluate the municipal wastes of Bilecik province in Turkey. The designed system includes a two-stage digester tank system for more effective biogas production, a Brayton cycle, and a thermal energy storage (TES) system integrated into the two heat exchanger networks for residential heating and domestic hot water. This study comprehensively investigates the Brayton cycle throughout

the combustion process. In this regard, the energy and exergy analyses were conducted to evaluate the thermodynamic system through the different biogas compositions, environmental conditions, and compression ratios (CR).

2. System description

The primary energy source of the proposed system model is biogas energy. The system consists of a biogas digestion area, a cogeneration cycle, and a waste heat subsystem. Although the integrated use of the energy sources requires the levelized use of energy according to its temperature grade (Arslan et al., 2021; Arslan and Kose, 2010), it is sometimes better to design the system according to the primary purpose of the use depending on the higher temperature grades (Arslan, 2021; Arslan et al., 2022). The primary purpose of the designed system is to produce biogas and generate power. The secondary purpose is the heat generation for domestic hot water and residential heating. In this regard, the system was designed to meet the required heat of the biogas production process through the waste heat of power generation. A schematic representation of the proposed system is given in Fig. 1. Municipal waste was evaluated as biomass input. These wastes consist of cattle manure, poultry manure and organic waste. Here, organic waste was accepted as kitchen waste.

A two-stage digester tank was evaluated for effective biogas production. The substrate, fermented for a certain period in the pre-digester unit, is transferred to the post-digester to continue fermentation. In this way, biogas production is increased by providing a longer fermentation process. The biogas continuously produced in the tanks is first sent to the desulfurisation unit. Since biogas typically contains around 0.05–0.3% hydrogen sulfide (H_2S), which has a corrosive impact on metals, there is a risk of causing harm to the engine and pipes (Akbulut et al., 2021). Therefore, for a better quality fuel, it must be separated from biogas in the desulfurisation unit. After this stage, biogas is sent to the cogeneration cycle. The air compressed in the compressor reacts with biogas in the CC. After combustion, the high temperature and pressure gas operate the turbine and generate power. Some of the heat of the gaseous fluid, which still has a high energy potential at the turbine exit, is used to keep the digester tanks at a suitable operating temperature. The remaining waste heat is stored in the thermal energy storage (TES) system. The stored heat can be utilised to meet the demand for hot water and to heat residences.

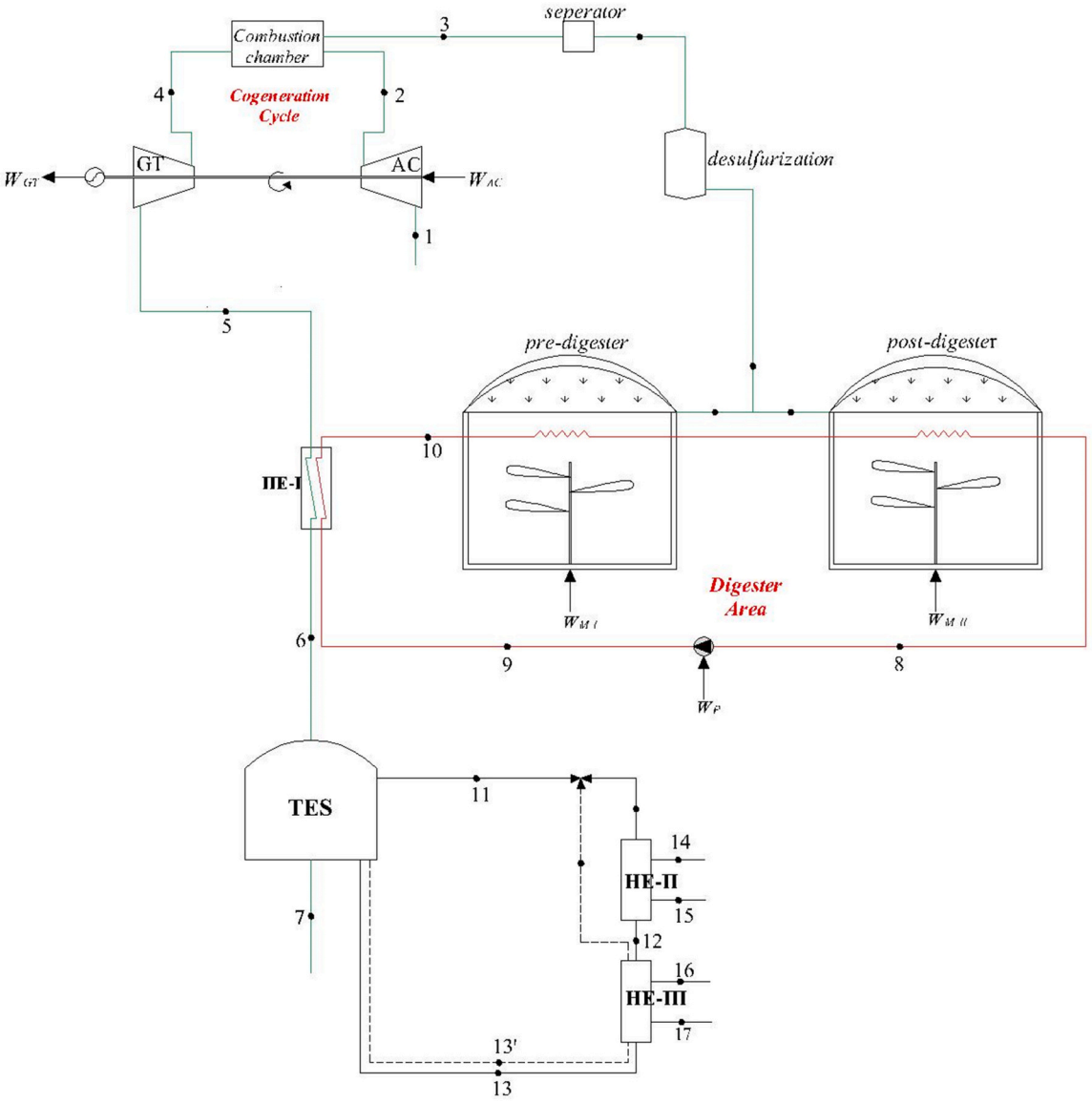

Fig. 1. Schematic diagram of the system.

3. Material and methods

The proposed system was evaluated thermodynamically through the energy and exergy analyses. In the study, the biogas production from the municipal waste of Bilecik province conducted. The produced biogas was later evaluated in a Brayton cycle power system. The combustion effects of the biogas on the Brayton cycle system were investigated along with the evaluation of the waste energy in the heating system for residential heating and domestic hot water. The following assumptions and limitations were handled in the analysis:

- Steady-state conditions are assumed.
- The terms kinetic and potential energy are neglected.
- T_0 and P_0 are 25 °C and 101.325 kPa, respectively.

- Air compressor (AC), gas turbine (GT), and pump (P) isentropic efficiency are %86, %86, and %95, respectively (Gholizadeh et al., 2019a, 2019b).
- Pressure drop in HE is assumed to be 10%.
- For effective heat transfer, the temperature difference of the HE is accepted as 15 ℃.
- CR rates were evaluated between 2-10.
- The ambient temperature was selected between -10–30 ℃.
- The CH_4 rate in biogas was handled, ranging between 60 % and 100 %.
- Biogas and air are handled as ideal gas at 40 °C.
- The air mixture consists of 21 % O_2 and 79 % N_2.

3.1. Biogas system

Biogas is a gas obtained due to the anaerobic fermentation of organic waste. The biomass must undergo preliminary preparation before being sent to the digester. The first stage of the preliminary process is to reduce the particle size. To avoid clogging installation elements such as pumps and pipes, the fluid and particle size of the solution must be minimal. It has been stated that the recommended particle size for effective biogas production is 0.008 mm and 0.4 mm (Abbasi et al., 2011). The next step is to obtain a homogeneous mixture. For this, biomass must be diluted with water. Waste types have different dilution rates because they have different chemical properties (Abbasi et al., 2011). In this study, the municipal wastes of Bilecik province were evaluated for biogas production. The information about the available average wastes is given in Table 1.

Biogas production according to the amount of waste is calculated as follows (Kaynarca et al., 2021):

$$V_{bio} = \sum m_m \bullet DM \bullet ODM \bullet \mu_{bio} \quad (1)$$

where V_{bio} and m_m are defined as the daily biogas production and the waste amount (tons/day), respectively. DM, ODM, and μ_{bio} are the amount of dry matter in wet manure (%), the amount of organic dry matter in dry matter (%) and biogas yield (lt/kg·ODM), respectively. The amount of methane gas produced is calculated using the amount of biogas production (Kaynarca et al., 2021):

Table 1
The properties of available wastes of Bilecik province (Environment and Urban Ministry EUM, 2017, Erikgenoglu, 2024).

Waste Type	Waste amount (tons/day)	DM (%)	ODM (%)	Dilution rate
Cattle waste	10	23	80	1:1
Poultry waste	20	55	75	1:3
Organic waste	20	18	90	-

$$V_{CH_4} = V_{bio} \bullet C_{CH_4} \quad (2)$$

where V_{CH_4} and C_{CH_4} are defined as the amount of methane gas and the percent (%) methane content, respectively. The accepted values for calculating biogas production and the amount of biogas obtained are given in Table 2.

A biogas plant comprises several key elements, including the digester tank, insulation material, mixer, pump, and pipes. After the preliminary preparation stage, the substrate sent to the reactor must be kept for a period called hydraulic retention time (HRT) to obtain biogas as a result of decay by bacteria. For the mesophilic temperature range, an HRT of 25–40 days is suitable (Garkoti et al., 2024). The first stage in digester tank design is to determine the tank volume according to the determined amount of manure and HRT. The volume of the digester tank is calculated as follows (Akbulut et al., 2021):

$$V_D = \left(m_m + \sum_{i=1}^{n} m_{csi}\right) \bullet HRT \quad (3)$$

where V_D is digester tank volume (m^3), and m_{csi} is the co-substrates quantity (tons/day). The diameter of the digester tank can be calculated as follows (Akbulut et al., 2021):

$$D^2 = \frac{4 \bullet V_D}{H \bullet \pi} \quad (4)$$

where D is diameter of the digester, and H is height of the digester. In this study, the diameter calculation was conducted, assuming a fixed height of the digester. It can determine the dimensions of the post-digestion storage using the following calculation (Akbulut et al., 2021):

$$V_{pds} = \left(m_m + \sum_{i=1}^{n} m_{csi}\right) \bullet \left(\frac{t_s}{12}\right) - V_D \quad (5)$$

where V_{pds} and t_s are post-digestion volume (m^3) and storage time. The volume of the biogas storage section is considered to be 5:1 of the total tank volume.

Reactor temperature is one of the most critical parameters affecting biogas production. The most suitable temperature for decay occurs under mesophilic conditions ranging between 20 and 40 °C (Vasan et al., 2024). In addition, mesophilic bacteria overreact at sudden temperature changes, so the reactor temperature must be stable. It is essential to insulate the reactor for a constant operating temperature. A cross-sectional representation of the digester tank is given in Fig. 2. The tank consists of three parts: the inner area (1), the concrete wall (2), and the insulation material (3).

The concrete wall and the insulation material (extruded polystyrene) have thermal conductivity coefficients of 0.79 W/m.K and 0.034 W/m.K, respectively (Cengel et al., 2011). Critical radius (r_{cr}) is an essential factor for determining the insulation material thickness and is calculated as follows:

$$r_{cr} = \frac{k_3}{h_a} \quad (6)$$

where k_3 and h_a (5 $W/m^2 \cdot K$) are the conductivity of insulation material and the convection coefficient of air (Cengel et al., 2011). Accordingly,

Table 2
Accepted values for calculating the amount of biogas (Environment and Urban Ministry EUM, 2017; Erikgenoglu, 2024).

Waste Type	μ_{bio} (lt/kg-ODM)	C_{CH_4} (%)	V_{bio} (m^3/day)
Cattle waste	450	55	828
Poultry waste	400	62	3300
Organic waste	700	60	2268
Total			**6396**

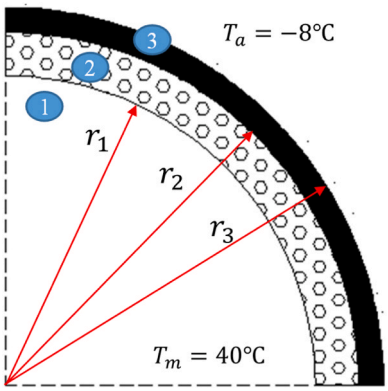

Fig. 2. Cross-section of the digester tank.

the r_{cr} was determined as 7 mm. Any insulation thickness selected above this value represents the appropriate insulation thickness for the tank. Therefore, considering the studies in the literature, the insulation thickness was accepted as 80 mm in view of the application of the literature (Akbulut et al., 2021). The design parameters of the digester tank are given in Table 3.

The illustration of the digester tank's physical model is provided in Fig. 3. The energy balance equation can be expressed as follows (Akbulut et al., 2021):

$$\rho_m \bullet V_m \bullet c_{p,m} \bullet \frac{dT_m}{dt} = \dot{Q}_{th} - \dot{Q}_m - \dot{Q}_D \tag{7}$$

where ρ, V_m and $c_{p,m}$ are the density of manure (kg/m^3), the volume of the digester (m^3), the specific heat of the manure (kJ/kg°C). $\dot{Q}_{th}$, $\dot{Q}_{m,}$ and $\dot{Q}_D$ are the rate produced heat energy delivered from the biogas (kW), rate of energy delivered to the incoming manure (kW), and total heat losses through the digester (kW).

The heat loss of the digester can be calculated as follows:

$$\dot{Q}_D = \frac{T_m - T_a}{\frac{1}{2\pi r_1 H h_1} + \frac{\ln(r_2/r_1)}{2\pi H k_2} + \frac{\ln(r_3/r_2)}{2\pi H k_3} + \frac{1}{2\pi r_3 H h_a}} \tag{8}$$

where T_m, T_a, $h_{1,}$ and k_2 define the manure temperature (°C), minimum ambient temperature (°C), convection coefficient of manure, and conductivity of concrete wall, respectively. The rate of energy delivered to the incoming manure can be calculated as follows:

$$\dot{Q}_m = \dot{m}_m \bullet c_{p,m} \bullet (T_m - T_a) \tag{9}$$

3.2. Brayton cycle

The Brayton cycle driven by biogas was taken into account in the system. First of all, fresh air in the environment is absorbed and compressed by the compressor. Different CRs were taken into account in the designed system. At the compressor outlet, the air, which is at high temperature and pressure, reacts with biogas in the CC. The reaction in the CC is given as (Arslan and Erbas, 2021):

Table 3
Design parameters of the digester tank.

Parameters	Value
Number of digesters	2
Height of the digester (H)	7 m
HRT	28 day
Operating temperature (T_m)	40 ℃
Ambient temperature (T_a)	-8 ℃
Thermal conductivity of insulation (k_3)	0.034 W/m.K
Thermal conductivity of the concrete wall (k_2)	0.79 W/m.K

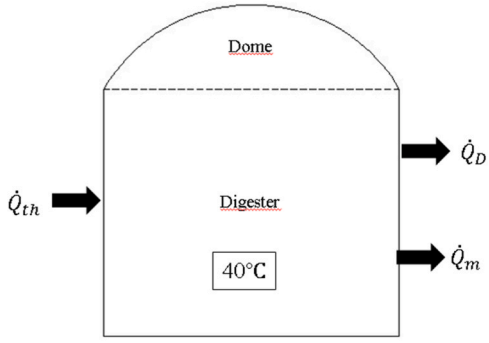

Fig. 3. The physical model of the digester tank.

$$\overbrace{a{\cdot}CH_4 + b{\cdot}CO_2}^{Fuel} + \overbrace{(1+\lambda){\cdot}\alpha_{th}{\cdot}(O_2 + 3.76N_2)}^{Air} \rightarrow \overbrace{xCO_2 + yH_2O + zO_2 + wN_2}^{Product} \tag{10}$$

where a and b are defined as methane (CH_4) and carbon dioxide (CO_2). λ, indicates the coefficient of excess air, α_{th}, air stoichiometric coefficient, x, y, z, and w are mole number of CO_2, H_2O, O_2 and N_2 in the products, respectively. The unknown values were determined by taking the mass balance into account λ was assumed as 250 % for a better combustion condition (Karaali and Ozturk, 2007). The high-temperature gases formed as a result of combustion expand in the turbine, generating power. While some of the heat of the gas fluid, which still has high energy potential at the turbine exit, is used to keep the digester tanks at optimum operating temperature, the remaining heat is stored in the TES system.

3.3. Heating system

The waste heat obtained from the Brayton cycle can be used for residential heating and hot water needs. While there is a constant demand for hot water throughout the year, the need for heating arises only during the winter months. A TES system was integrated into the system to meet the required heat for both of these situations. Thanks to the TES system, waste heat is stored in the tank. While this heat is used for both hot water and domestic heating in the winter months, it is used only to meet the hot water needs in the summer months. The heat need of a residence is determined as follows:

$$\dot{Q}_{demand} = U \bullet A \bullet \Delta T \tag{11}$$

where U and A are defined the heat transfer coefficient and heat transfer area of the building structures (such as window, floor, ceiling, and wall), and ΔT is temperature difference between indoor and outdoor. The U values were determined in accordance with the Turkish Standards Institution (TS825, 2008). Accordingly, U and A values of building structures were accepted as given in Table 4. According to these assumptions, the heat demand of the residences was calculated, assuming that the heating process would start if the daily average ambient temperatures were less than 15 °C. For residential heating, the inlet and outlet temperatures of water were accepted as 50 ℃ and 60 ℃, respectively (Hu et al., 2024).

Table 4
The heat transfer coefficient and heat transfer area of building structures (Arslan and Arslan, 2022).

Structures	U (W/m^{2}K)	A (m^2)
Wall	0.5	100
Floor	2.4	100
Window	0.45	20
Ceiling	0.3	100

Daily ambient temperatures were calculated using data obtained from the general directorate of meteorology (General Directorate of Meteorology GDM, 2023). Fig. 4 shows the daily average ambient temperatures and daily heat demand variation of a residence. Considering the environmental conditions of the coldest day (-8 ℃), the required heat demand for a residence was determined to be 5.3 kW.

The need for hot water for the residences was met by heating the province network water. So, the inlet temperature was accepted as 10 ℃, and the hot water temperature used in residences was determined as 50℃ (Zendehboudi, 2024; Hu et al., 2024). In this study, it was assumed that four people lived in a residence. Accordingly, the daily hot water requirement of a residence is 150 litres/day (Boz and Mutlu, 2013).

3.4. Energy and exergy analysis

In steady-state conditions, the mass balance is described by considering the rates at which mass enters and exits the system:

$$\Sigma \dot{m}_i = \Sigma \dot{m}_o \tag{12}$$

where $\dot{m}_i$ and $\dot{m}_o$ are the mass flow rates at the inlet and outlet, respectively. In a continuous flow system, the principle of transferring energy can be expressed through an equation that accounts for the energy transferred through heat, work, and mass:

$$\dot{Q} + \dot{W} = \Sigma \dot{m}_o h_o - \Sigma \dot{m}_i h_i \tag{13}$$

where $\dot{Q}$ is the heat transfer rate and $\dot{W}$ is the power, h_i and h_o are specific enthalpies at inlet and outlet. the energy balance of the-combustion is given as (Cengel and Boles, 1994):

$$\dot{Q}_f = \sum_i \dot{n}\left(\overline{h}_0^f + \overline{h}_T - \overline{h}_{298}\right) - \sum_o \dot{n}\left(\overline{h}_0^f + \overline{h}_T - \overline{h}_{298}\right) \tag{14}$$

where $\dot{Q}_f$ describes the heat of fuel. $\dot{n}$, $\overline{h}_0^f$, $\overline{h}_T$ and $\overline{h}_{298}$ are mole ratio, enthalpy of formation, enthalpy at the temperature T, and enthalpy at 298 K. The exergy balance for the k^{th} component of the system (Cengel and Boles, 1994):

$$\dot{E}x_k^Q - \dot{E}x_k^W - \sum(\dot{m}_i\psi_i)_k - \sum(\dot{m}_o\psi_o)_k - \dot{E}x_{d,k} = 0 \tag{15}$$

where $\dot{E}x_{i,k}$ and $\dot{E}x_{o,k}$ are the exergy inlet and outlet to the k^{th} component, $\dot{E}x_{d,k}$ is the exergy destruction rate. $\dot{E}x_k^Q$, $\dot{E}x_k^W$ and ψ are describe the exergy of heat, the exergy of work and the specific exergy flow, respectively, and are given (Cengel and Boles, 1994):

$$\dot{E}x_k^Q = \left(1 - \frac{T_0}{T}\right)Q_k \tag{16}$$

$$\dot{E}x_k^W = \dot{W}_k \tag{17}$$

$$\psi = (h - h_0) - T_0(s - s_0) \tag{18}$$

where, s is define entropy. For the combustion process exergy balance can be given as (Ucar and Arslan, 2021, Arslan and Erbas, 2021):

$$\dot{E}x_f = \left(1 - \frac{T_0}{T_{cc}}\right) - I \tag{19}$$

where I describes the exergy destruction rate and is given as (Cengel and Boles, 1994):

$$I = T_0 S_g \tag{20}$$

$$S_g = S_0 - S_i + \frac{\dot{Q}_f}{T_{cc}} \tag{21}$$

where S_g is general entropy of fuel-air mixture and are given by the following equation:

$$S_k = \sum_o \dot{n}_k(\overline{s}_k^o(T, P_0) - R_u \ln(x_k P)) \tag{22}$$

where $\overline{s}_k^o$, R_u, x_k and P are define molar entropy of the k^{th} component, universal gas contant (8.314 kJ/kmole.K), mole ratio of the k^{th} compound and total pressure of the flow. The energy and exergy balance equations for each component are detailed in Table 5.

Energy efficiency (η) and exergy efficiency (ε) of the overall system are established as follows:

$$\eta = \frac{\dot{W}_{net} + \dot{Q}_h}{\dot{Q}_f} \tag{23}$$

$$\varepsilon = \frac{\dot{W}_{net} + \dot{E}x_{\dot{Q}_h}}{\dot{E}x_{\dot{Q}_f}} \tag{24}$$

where, $\dot{W}_{net}$ is the net electrical power in the system and is calculated as follows:

$$\dot{W}_{net} = \dot{W}_{GT} - \dot{W}_{AC} - \dot{W}_P - \dot{W}_{M-I} - \dot{W}_{M-II} \tag{25}$$

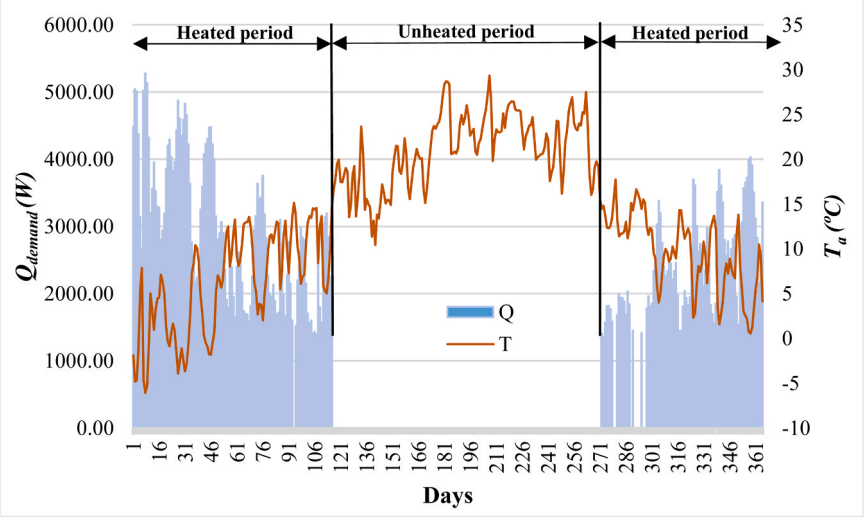

Fig. 4. Variation of ambient temperature and heat demand of residences.

Table 5
Details of energy and exergy balance equations for each component.

Component	Energy balance equations	Exergy balance equations
AC	$\dot{W}_{AC} = \dot{m}_{air}(h_2 - h_1)$, $\eta_{AC} = \frac{h_1 - h_{2s}}{h_1 - h_2}$	$\dot{E}x_{d,AC} = \dot{W}_{AC} - \left(\dot{E}x_2 - \dot{E}x_1\right)$
CC	$Q_{cc} - \dot{E}_2 - \dot{E}_3 + \dot{E}_4 = 0$	$\dot{E}x_{d,cc} = \dot{E}x_2 + \dot{E}x_3 - \dot{E}x_4 - \dot{E}x^{Q_{cc}}$
GT	$\dot{W}_{GT} = \dot{m}_{prod}(h_4 - h_5)$, $\eta_{GT} = \frac{h_4 - h_5}{h_4 - h_{5s}}$	$\dot{E}x_{d,GT} = \dot{E}x_4 - \dot{E}x_5 - \dot{W}_{GT}$
HE-I	$\dot{m}_{prod}h_5 + \dot{m}_w h_9 = \dot{m}_{prod}h_6 + \dot{m}_w h_{10}$	$\dot{E}x_{d,HE-I} = \dot{E}x_5 + \dot{E}x_9 - \dot{E}x_6 - \dot{E}x_{10} - \dot{E}x_{Q,HE-I}$
P	$\dot{W}_P = \dot{m}_w(h_9 - h_8)$, $\eta_P = \frac{h_{9s} - h_8}{h_9 - h_8}$	$\dot{E}x_{d,P} = \dot{W}_P - \left(\dot{E}x_9 - \dot{E}x_8\right)$
HE-II	$\dot{m}_w h_{11} + \dot{m}_h h_{14} = \dot{m}_w h_{12} + \dot{m}_h h_{15}$	$\dot{E}x_{d,HE-II} = \dot{E}x_{11} + \dot{E}x_{14} - \dot{E}x_{12} - \dot{E}x_{15} - \dot{E}x_{Q,HE-II}$
HE-III	$\dot{m}_w h_{11} + \dot{m}_d h_{16} = \dot{m}_w h_{13} + \dot{m}_d h_{17}$	$\dot{E}x_{d,HE-III} = \dot{E}x_{11} + \dot{E}x_{16} - \dot{E}x_{13} - \dot{E}x_{17} - \dot{E}x_{Q,HE-III}$

where $\dot{W}_{GT}$ is the power generated in the gas turbine, $\dot{W}_{AC}$, $\dot{W}_P$, $\dot{W}_{M-I}$ and $\dot{W}_{M-II}$ are defined as the power required for air compressor, pump, and mixers. The required power for mixers was accepted as 11 kW (Akbulut et al. 2021).

4. Results

In the first stage of this study, the design of the digestion area was conducted. The necessary digestion tank and biogas storage volume were determined based on the daily amounts of municipal waste. The second part of the research involves the analysis of a cogeneration cycle. Here, the incoming air to the compressor is compressed at specified ratios. The air compressed in the compressor reacts with biogas in the CC. The high-temperature and high-pressure gas flow drives a turbine to generate power. Some of the energy of the gas, still possessing a high energy potential at the turbine outlet, is utilised to maintain the biogas digestion tanks at a constant temperature. The remaining heat is stored in the TES tank. It is used to meet the hot water demand of residences during the summer and the hot water and heating demand of residences in the winter. The size of the digester tanks was determined by considering the daily waste amount and *HRT*. Accordingly, the required tank diameter for a digester tank with a height of 7 m was determined to be 20 m. The $\dot{V}_D$ and V_{pds} are 1300 m^3 or 780 m^3, respectively. In addition, the biogas storage volumes of these tanks are 260 m^3 and 156 m^3, respectively. As the thickness of the insulation material increases, heat loss decreases to a certain extent, but after a certain point, heat loss to the environment begins. This point is called the critical radius and was calculated as 7 mm in this study. Any insulation thickness selected above this value represents the appropriate insulation thickness for the tank. Therefore, considering the studies in the literature, the insulation thickness was accepted as 80 mm.

The designed system was thermodynamically analysed under five different CR, varying amounts of CH_4 gas, and different T_a. The change of T_a and CR has a significant impact on energy and exergy efficiency. In Fig. 5, variations in η and ε values under the combustion condition with 100 % CH_4 are presented for different CR.

According to Fig. 5, it was observed that η and ε increase with the increase of the environmental temperature at different CR values. However, it was observed that the efficiencies decrease as the CR increases depending on the increase in the compression power. When the CR was 10, and the T_a was 263.15 K, the lowest η and ε were determined to be 31.96 % and 24.32 %, respectively. The highest η and ε were respectively determined to be 43.40 % and 41.25 % when CR was 2, and the T_a was 303.15 K. In Fig. 6, the variation in η and ε values under the combustion condition with 80 % CH_4 are presented for different CRs.

According to Fig. 6, it was observed that η and ε increase with the increase of the environmental temperature at different CR values. However, it was observed that the efficiencies decrease as the CR increases depending on the increase in the compression power. When the CR was 10, and the T_a was 263.15 K, the lowest η and ε were determined to be 32.03 % and 24.40 %, respectively. The highest η and ε were respectively determined to be 43.22 % and 40.97% when CR was 2, and the T_a was 303.15 K. In Fig. 7, the variation in η and ε values under the combustion condition with 60% CH_4 are presented for different CRs.

According to Fig. 7, it was observed that η and ε increase with the increase of the environmental temperature at different CR values. However, it was observed that the efficiencies decrease as the CR increases depending on the increase in the compression power. When the CR was 10, and the T_a was 263.15 K, the lowest η and ε were determined to be 31.74 % and 23.85 %, respectively. The highest η and ε were respectively determined to be 42.75 % and 40.17 %% when CR was 2,

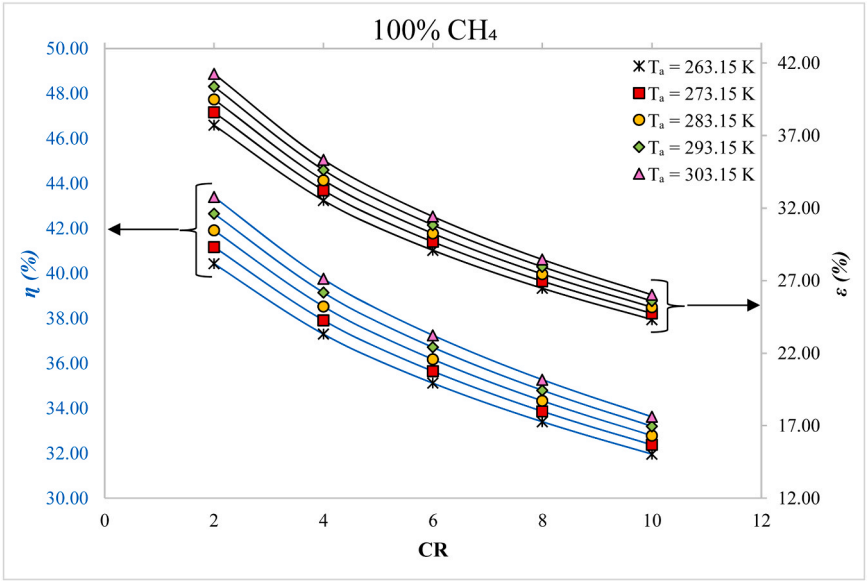

Fig. 5. Effect of compression ratio on η and ε in case of 100 % CH_4.

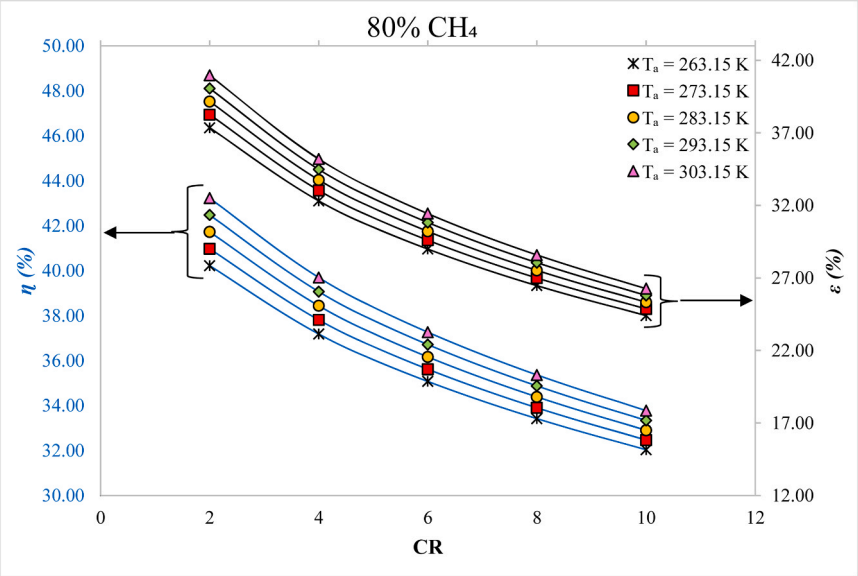

Fig. 6. Effect of compression ratio on η and ε in case of 80 % CH_4.

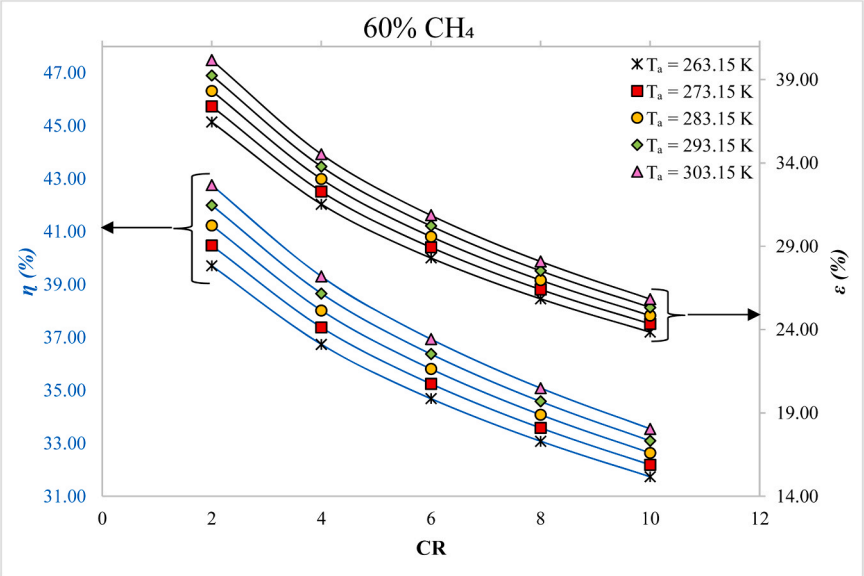

Fig. 7. Effect of compression ratio on η and ε in case of 60 % CH_4.

and the T_a was 303.15 K. When the efficiency values obtained at different methane rates are examined, it can be said that the increase in methane gas rate increases the system efficiency, as expected. Similarly, the increase in ambient temperature also has a positive effect on the system efficiency. The ambient temperature also affects the product temperature (T_4) since it enhances the combustion process. The variation of T_4 versus CR for different T_a values is shown in Fig. 8.

Fig. 8 shows the variation of T_4 with respect to ambient temperature at different CH_4 rates and different CRs. When examining the variation in T_4 resulting from the combustion of 100 % CH_4 based on T_a and CR, it was found that the highest T_4 was 1259.02 K when the T_a was 303.15 K and the CR was 10. Similarly, the lowest T_4 for the same CH_4ratio was determined to be 1040.57 K when the T_a was 263.15 K and the CR was 2. When examining the variation in T_4 resulting from the combustion of 80 % CH_4 based on T_a and CR, it was found that the highest T_4 was 1256.35 K when the T_a was 303.15 K and the CR was 10. Similarly, the lowest T_4 for the same CH_4ratio was determined to be 1034.72 K when the T_a was 263.15 K and the CR was 2. When examining the variation in T_4 resulting from the combustion of 60 % CH_4 based on T_a and CR, it was found that the highest T_4 was 1244.48 K when the T_a was 303.15 K and the CR was 10. Similarly, the lowest T_4 for the same CH_4ratio was determined to be 1021.95 K when the T_a was 263.15 K and the CR was 2. These results show that the combustion process is significantly affected by factors such as ambient conditions and CRs.

The net power production obtained from the system and the amount of heat storage in the TES system were examined at different methane gas rates. Accordingly, Fig. 9 shows the $\dot{W}_{net}$ and $\dot{Q}$ in case of 100 % CH_4.

When Fig. 9 is examined, it is seen that power generation increases directly proportional to the T_a and inversely proportional to the CR. Accordingly, the lowest power generation was determined as 572.47 kW when the CR was 10 and T_a was 263.15 K. The highest power generation was determined as 876 kW when the CR was 2 and the T_a was 303.15 K. Since waste heat is stored in the TES system, it has been

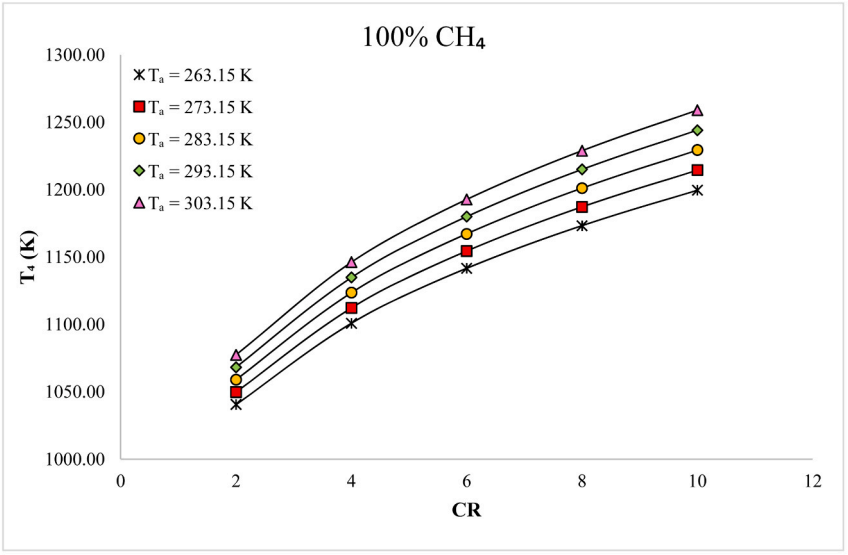

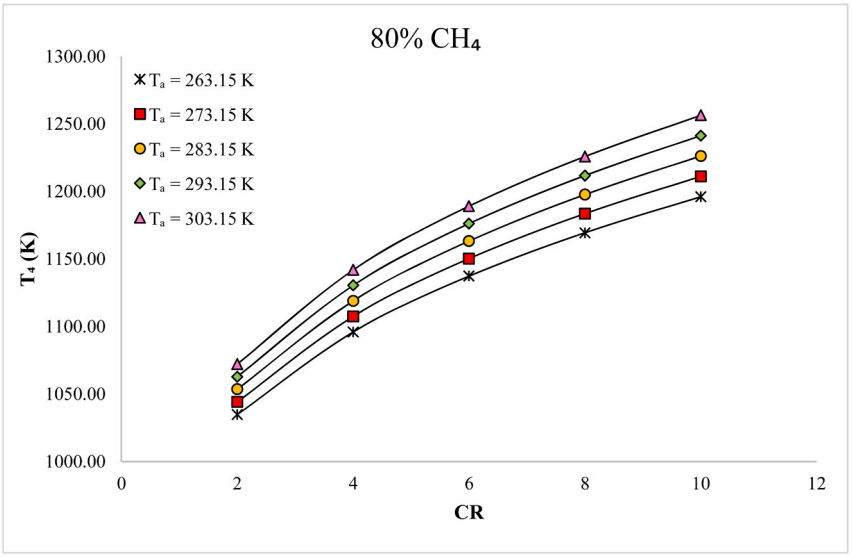

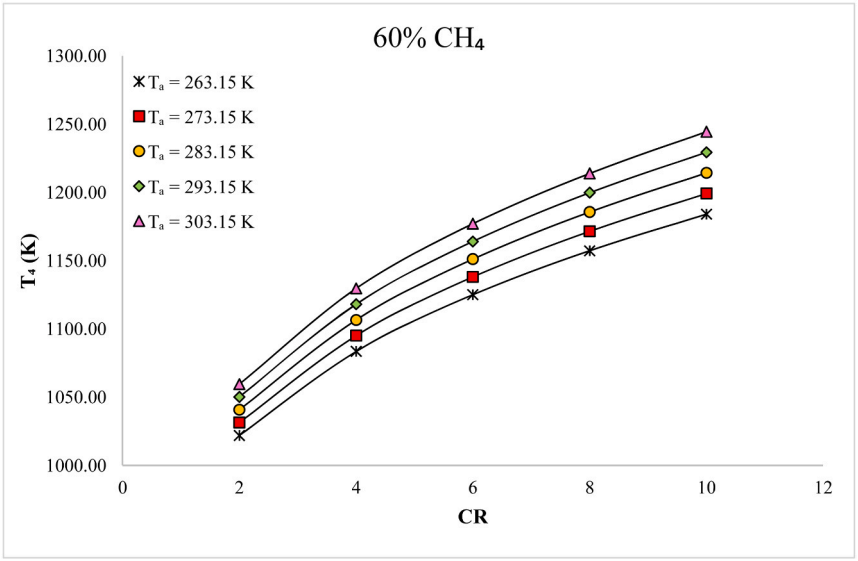

Fig. 8. Effect of compression ratio on the product temperature.

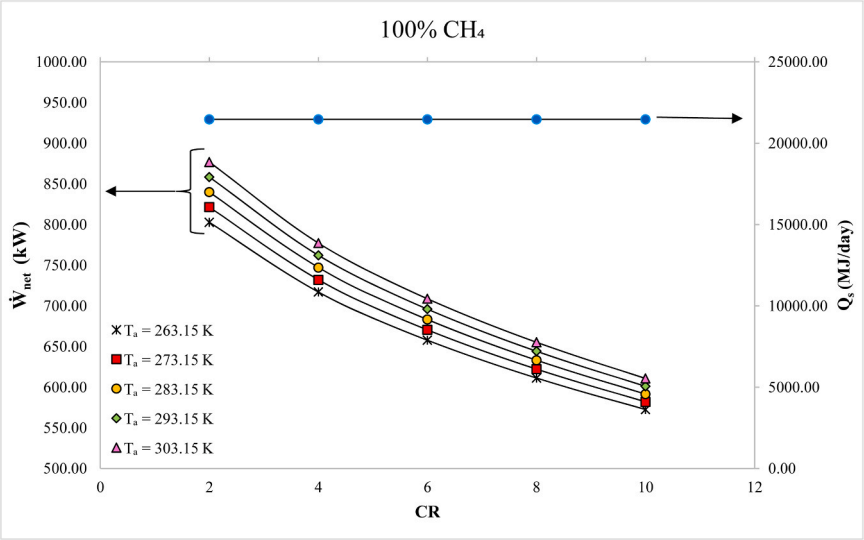

Fig. 9. . $\dot{W}_{net}$ and $\dot{Q}$ values in case of 100 % CH_4.

determined that this heat remains constant and it has been determined that 21470.86 MJ/day of heat can be stored daily from this system. Fig. 10 shows the $\dot{W}_{net}$ and $\dot{Q}$ in case of 80 % CH_4.

When Fig. 10 is examined, it is seen that power generation increases directly proportional to the T_a and inversely proportional to the CR. Accordingly, the lowest power generation was determined as 463.19 kW when the CR was 10 and the T_a was 263.15 K. The highest power generation was determined as 699.95 kW when the CR was 2 and the T_a was 303.15 K. Since waste heat is stored in the TES system, it has been determined that this heat remains constant,and it has been determined that 17340.4 MJ/day of heat can be stored daily from this system. Fig. 11 shows the $\dot{W}_{net}$ and $\dot{Q}$ in case of 60 % CH_4.

When Fig. 11 is examined, it is seen that power generation increases directly proportional to the T_a and inversely proportional to the CR. Accordingly, the lowest power generation was determined as 342.49 kW when the CR was 10 and the T_a was 263.15 K. The highest power generation was determined as 514.73 kW when the CR was 2 and the T_a was 303.15 K. Since waste heat is stored in the TES system, it has been determined that this heat remains constant and it has been determined that13209.9 MJ/day of heat can be stored daily from this system. The heat stored in the TES system can be used for both domestic heating and hot water needs in winter, while it can only be used for hot water needs in summer. Fig. 12 shows how many residences can benefit from the heat stored in the TES system under operating conditions where different methane gas rates are examined.

When Fig. 12 is examined, it is determined that the domestic hot water (DHW) needs of 1136, 917, and 699 residences can be met from the waste heat obtained under the system conditions where 100 % CH_4, 80 % CH_4, and 60 % CH_4 are burned, respectively. Similarly, under system conditions where 100 % CH_4, 80 % CH_4, and 60 % CH_4 are burned, it was determined that the waste heat obtained could provide both residence heating (RH) and DHW for 565, 457, and 348 residences, respectively. Accordingly, the DHW and RH needs of more residences can be met thanks to the heat obtained by burning %100 CH_4.

According to the analysis, it was determined that the system provided the best operating conditions when CR, CH_4 rate, and T_a values were 2, 100 %, and 303.15, respectively. In this case, η, ε, and $\dot{W}_{net}$ are calculated as 43.40 %, 41.25 % and 876.83 kW, respectively. In addition, it was determined that the DHW needs of 1136 residences and both DHW and RH of 565 residences could be met with the waste heat

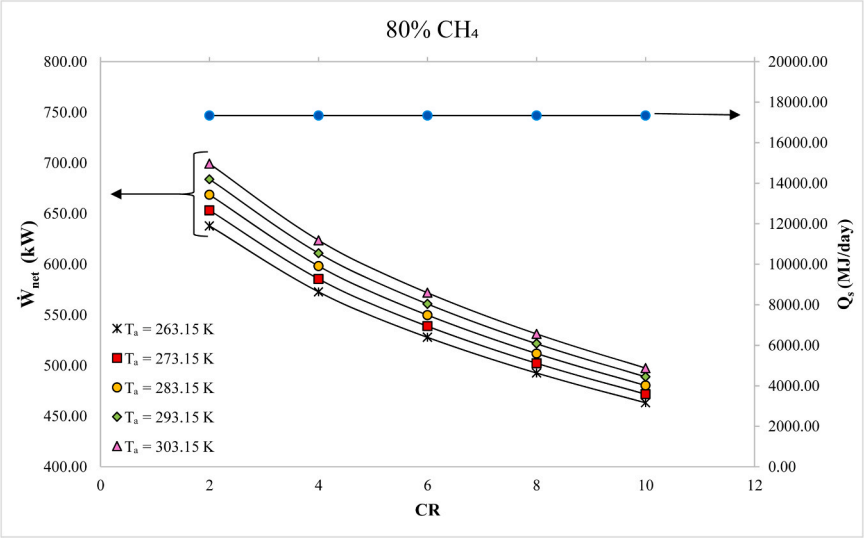

Fig. 10. . $\dot{W}_{net}$ and $\dot{Q}$ values in case of 80 % CH_4.

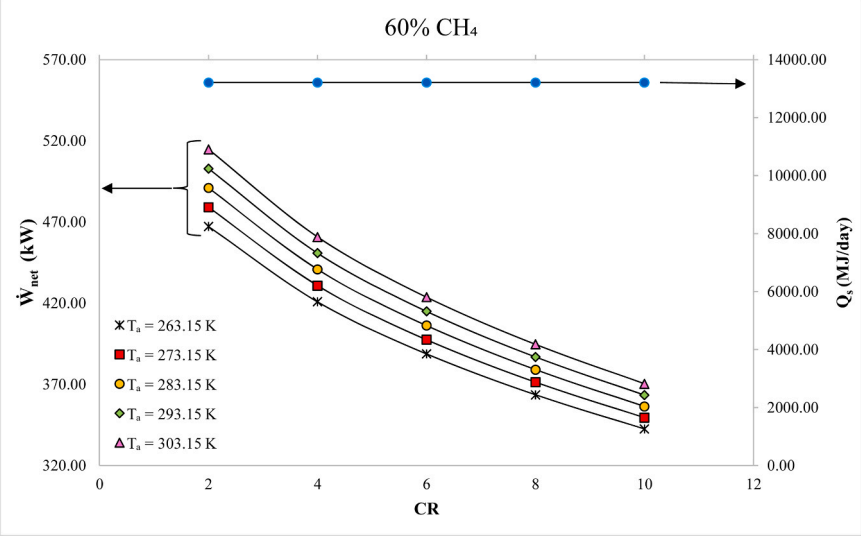

Fig. 11. . $\dot{W}_{net}$ and $\dot{Q}$ values in case of 60 % CH_4.

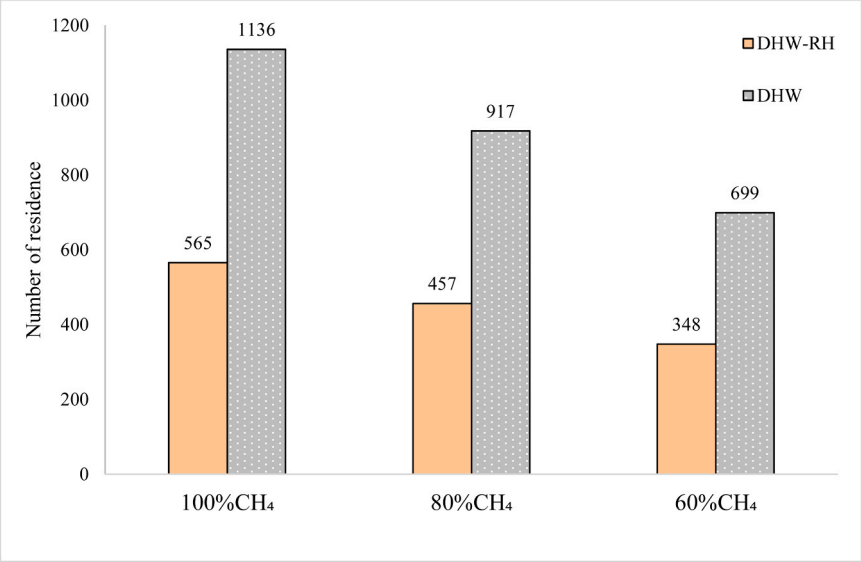

Fig. 12. Number of residences benefiting from the heat stored in the TES system according to different methane gas rates.

obtained from the system under these conditions. The thermodynamic properties of each point of this cycle are given in Table 6.

The results of energy and exergy analyses for each component in the system are presented in Table 7. When the results are examined, the 100 % CH_4 ratio leads to a more efficient combustion process. This situation also increased the product temperature, contributing to higher power generation and heat gain. So, it would be better to separate the formed CO_2 from the biogas before the combustion.

As a result, when the system was examined in terms of energy and exergy efficiencies, it was determined that the gas containing 100 % CH_4 gave the best results at all parameter values. Accordingly, it can be said that by separating the gas from CO_2, the net power generation obtained from the system will also increase. Similarly, due to the increase in the amount of stored waste heat, the DHW and RH needs of more residences can be met. When the system is examined through the change in CR, the combustion temperature also increases as the CR increases, and the power generation in the gas turbine increases. However, as the increase in CR also increases the power required for the air compressor, a decrease in the net power of the system is observed.

Table 6
Thermodynamic properties at each point of the system.

Point	$\dot{m}$ (kg/s)	T (K)	P (kPa)	$\dot{E}$ (kW)	$\dot{E}x$ (kJ/kg)
1	3.18	303.15	101.3	970.32	6536.63
2	3.18	380.51	202.65	1219.85	6791.13
3	0.053	313.15	–	50.02	107.29
4	3.23	1077.44	204.68	3863.05	9505.94
5	3.23	729.53	200	2541.71	8184.59
6	3.23	373.15	180	1289.50	6932.34
7	3.23	298.15	101.3	1035.92	6678.61
8	2.82	318.15	35	530.48	7.538
9	2.82	318.45	50	534.01	7.775
10	2.82	335.01	45	943.05	53.476
11	0.26	348.15	–	82.58	4.16
12	0.26	343.25	–	77.19	3.41
13	0.26	313.15	–	44.07	0.40
14	0.127	323.15	–	26.52	0.53
15	0.127	333.15	–	31.82	1.01
16	0.0017	283.15	–	0.073	1.61
17	0.0017	323.15	–	0.292	1.52

Table 7
Energy and Exergy analyses results of system components.

Component	$\dot{Q}$ (kW)	$\dot{W}$ (kW)	$\dot{E}x_Q$ (kW)	$\dot{E}x_W$ (kW)	$\dot{E}x_d$ (kW)	η %	ε %
AC	–	290.15	–	290.15	48.98	98.78	96.78
CC	46.50	–	33.63	–	2573.88	44.27	67.29
GT	–	1136.35	–	1136.35	184.99	41.23	78.16
HE-I	25.04	–	14.81	–	1100.57	98	85.70
HE-II	0.10	–	0.014	–	0.296	98.14	97.72
HE-III	5.40	–	0.776	–	1.574	97.82	87.36
P	–	13.24	–	13.24	12.57	98.84	64.65
Overall system						43.40	41.25

5. Conclusions

This study presents a thermodynamic analysis of the biogas-driven cogeneration cycle. The primary purpose of the article is to examine biogas at different methane rates and evaluate the waste heat obtained from the cogeneration cycle. In the examined system, in addition to different methane gas rates, the CR of the compressor and ambient temperature changes were also taken into account. Accordingly, the main conclusions obtained in this study can be listed as follows:

- It is possible to produce 6396 m^3/day of biogas from municipal waste.
- In the case of the utilisation of biogas containing pure methane in the Brayton cycle, it is possible to generate 876.83 kW of power.
- It is possible to store 21470.86 MJ/day of heat from the waste heat obtained by the combustion of pure methane.
- The energy and exergy efficiency of the system are 43.40 % and 41.25 %, respectively.
- It is possible for the heat obtained to meet both the domestic hot water and residence heating needs of 565 residences in winter and the domestic hot water needs of 1136 residences in summer.

This study examines biogas production from municipal wastes in Bilecik province and evaluates its use in the cogeneration system. The system includes a Brayton cycle for power generation and a TES unit for heat storage to be used in the domestic hot water and residence heating through the two separate heat exchanger networks. However, there is still waste heat that needs to be used. So, a proton exchange membrane electrolyser unit can be evaluated in the designed system. Moreover, the O2 produced in the electrolyser can be used in the boiler for better combustion processes. The produced H_2 in the electrolyser can be stored or used as green biogas (mixing it with the CH_4) in the boiler for a better combustion process. Another future prospect can be called the integration of the proposed system with renewable energy sources such as solar energy.

CRediT authorship contribution statement

Oğuz Arslan: Conceptualization, Data curation, Formal analysis, Investigation, Methodology, Supervision, Writing – review & editing. **Damla Kilic Erikgenoglu:** Conceptualization, Data curation, Formal analysis, Investigation, Methodology, Writing – original draft.

Declaration of Competing Interest

The authors declare that they have no known competing financial interests or personal relationships that could have appeared to influence the work reported in this paper.

References

Abbasi, T., Tauseef, S.M., Abbasi, S.A., 2011. Biogas energy, vol. 2. Springer Science & Business Media.

Akbulut, A., Arslan, O., Arat, H., Erbaş, O., 2021. Important aspects for the planning of biogas energy plants: malatya case study. Case Stud. Therm. Eng. 26, 101076.

Anvari, S., Szlęk, A., Arteconi, A., Desideri, U., Rosen, M.A., 2023. Comparative study of steam injection modes for a proposed biomass-driven cogeneration cycle: performance improvement and CO_2 emission reduction. Appl. Energy 329, 120255.

Arslan, O., Acikkalp, E., Genc, G., 2022. A multi-generation system for hydrogen production through the high-temperature solid oxide electrolyzer integrated to 150 MW coal-fired steam boiler. Fuel 315, 123201.

Arslan, A.E., Arslan, O., Kandemir, S.Y., 2021. AHP–TOPSIS hybrid decision-making analysis: simav integrated system case study. J. Therm. Anal. Calor. 145, 1191–1202.

Arslan, O., Arslan, A.E., 2022. Pareto principle-based advanced exergetic evaluation of geothermal district heating system: simav case study. J. Build. Eng. 58, 105035.

Arslan, O., 2021. Performance analysis of a novel heat recovery system with hydrogen production designed for the improvement of boiler effectiveness. Int. J. Hydrog. Energy 46, 7558–7572.

Arslan, O., Erbas, O., 2021. Investigation on the improvement of the combustion process through hybrid dewatering and air pre-heating process: a case study for a 150 MW coal-fired boiler. J. Taiwan Inst. Chem. Eng. 121, 229–240.

Arslan, O., Kose, R., 2010. Exergoeconomic optimization of integrated geothermal system in Simav. Kutahya. Energy Convers. Manag. 51, 663–676.

Bai, H., Lin, H., Chauhan, B.S., Amer, A.M., Fayed, M., Ayed, H., Truong, N., 2023. Development of a novel power and freshwater cogeneration plant driven by hybrid geothermal and biomass energy. Case Stud. Therm. Eng. 52, 103695.

Barua, V.B., Kalamdhad, A.S., 2019. Biogas production from water hyacinth in a novel anaerobic digester: a continuous study. Process Saf. Environ. Prot. 127, 82–89.

Benato, A., Macor, A., 2017. Biogas engine waste heat recovery using organic rankine cycle. Energies 10 (3), 327.

Boz, B.E., Mutlu, N., 2013. Production of domestic hot water in residential buildings; options and comparisons. Process Eng. J. 133, 35–52.

Campero, L.A.C., Wang, W., Martin, A., 2023. Thermodynamic and exergetic analyses of a biomass-fired Brayton-Stirling cogeneration cycle for decentralized, rural applications. Energy Convers. Manag. 292, 117350.

Cao, Y., Dhahad, H.A., Togun, H., Haghghi, M.A., Anqi, A.E., Farouk, N., Rosen, M.A., 2021. Seasonal design and multi-objective optimization of a novel biogas-fueled cogeneration application. Int. J. Hydrog. Energy 46 (42), 21822–21843.

Cengel, Y.A., Boles, M.A., 1994. Thermodynamics: an Engineering Approach. McGraw Hill Inc, New York.

Cengel, Y.A., Tanyildizi, V., Dagtekin, İ., 2011. Heat and Mass Transfer. Guven Bookstore.

Environment and Urban Ministry (EUM), 2017. Biogas production from animal manure. ⟨https://www.csb.gov.tr/⟩ (Last access: July, 2023).

Erikgenoglu, D., 2024. Investigation of the Use of Bilecik Solar Energy Potential in Multigeneration Systems. Graduate Education Institute, Bilecik Seyh Edebali University (Ongoing Ph.D. dissertation).

Garkoti, P., Ni, J.Q., Thengane, S.K., 2024. Energy management for maintaining anaerobic digestion temperature in biogas plants. Renew. Sustain. Energy Rev. 199, 114430.

General Directorate of Meteorology (GDM), 2023. Ministery of Agriculture and Forestry of Turkish Republic. Official statistics, ⟨https://www.mgm.gov.tr/veridegerlendirme/il-ve-ilceler-istatistik.aspx?m=BILECIK⟩. (Last access: June, 2023).

Gholizadeh, T., Vajdi, M., Mohammadkhani, F., 2019a. Thermodynamic and thermoeconomic analysis of basic and modified power generation systems fueled by biogas. Energy Convers. Manag. 181, 463–475.

Gholizadeh, T., Vajdi, M., Rostamzadeh, H., 2019b. A new biogas-fueled bi-evaporator electricity/cooling cogeneration system: exergoeconomic optimization. Energy Convers. Manag. 196, 1193–1207.

Holik, M., Živić, M., Virag, Z., Barac, A., Vujanović, M., Avsec, J., 2021. Thermo-economic optimization of a Rankine cycle used for waste-heat recovery in biogas cogeneration plants. Energy Convers. Manag. 232, 113897.

Huang, Z., Su, B., Wang, Y., Yuan, S., Huang, Y., Li, L., Cai, J., Chen, Z., 2024. A novel biogas-driven CCHP system based on chemical reinjection. Energy 297, 131238.

Hu, Y., Luo, K., Zhao, D., Wu, Z., Yang, Y., Luo, E., Xu, J., 2024. Thermoacoustic heat pump utilizing medium/low-grade heat sources for domestic building heating. Energy Built Environ. 5 (4), 628–639.

Jabari, F., Arasteh, H., Sheikhi-Fini, A., Ghaebi, H., Bannae-Sharifian, M.B., Mohammadi-Ivatloo, B., Mohammadpourfard, M., 2022. A biogas-steam combined cycle for sustainable development of industrial-scale water-power hybrid microgrids: design and optimal scheduling. Biofuels, Bioprod. Bioref. 16 (1), 172–192.

Karaali, R., Ozturk, I.T., 2007. A review on improvement efficiency of gas turbine cogeneration systems. Eng. Mach. 49 (577), 16–21.

Kaynarca, H., Kilic, T., Acikkalp, E., Kandemir, S.Y., 2021. Assessment of biogas potential in Eskisehir. J. Geogr. (42), 271–282.

Kour, G., Basak, N., Kumar, S., 2024. State-of-the-art techniques to enhance biomethane/biogas production in thermophilic anaerobic digestion. Process Saf. Environ. Prot. 186, 104–117.
Lin, H., Liu, J., Ifseisi, A.A., Taghavi, M., 2023. A novel bio-waste-driven multigeneration cycle integrated with a solar thermal field and atmospheric water harvesting cycle: an effort to mitigate the environmental impacts of the wastewater treatment plants. Process Saf. Environ. Prot. 180, 386–403.
Mahmoodi-Eshkaftaki, M., Ebrahimi, R., 2019. Assess a new strategy and develop a new mixer to improve anaerobic microbial activities and clean biogas production. J. Clean. Prod. 206, 797–807.
Seirafi, F., Ebrahimi, R., Ghaebi, H., Bayareh, M., 2024. Pinch, energy, and exergy analysis for a power-hydrogen cogeneration system fueled by biogas. Process Saf. Environ. Prot. 183, 1223–1238.
Su, B., Han, W., He, H., Jin, H., Chen, Z., Yang, S., 2020. A biogas-fired cogeneration system based on chemically recuperated gas turbine cycle. Energy Convers. Manag. 205, 112394.
TS825, 2008. Thermal Insulation Requirements for Buildings. Turkish Standards Institution Ankara, Turkey.
Ucar, M., Arslan, O., 2021. Assessment of improvement potential of a condensed combi boiler via advanced exergy analysis. Therm. Sci. Eng. Prog. 23, 100853.
Vasan, V., Sridharan, N.V., Feroskhan, M., Vaithiyanathan, S., Subramanian, B., Tsai, P. C., Lin, Y.C., Lay, C.H., Wang, C.T., Ponnusamy, V.K., 2024. Biogas production and its utilization in internal combustion engines-a review. Process Saf. Environ. Prot. 186, 518–539.
Zare, A.D., Saray, R.K., Mirmasoumi, S., Bahlouli, K., 2019. Optimization strategies for mixing ratio of biogas and natural gas co-firing in a cogeneration of heat and power cycle. Energy 181, 635–644.
Zendehboudi, A., 2024. Energy, exergy, and exergoeconomic analyses of an air source transcritical CO_2 heat pump for simultaneous domestic hot water and space heating. Energy 290, 130295.
Zhang, Q., Yang, Y., Hou, L.A., Zhu, H., Zhang, Y., Pu, J., Li, Y., 2023a. Recent advances of carbon-based additives in anaerobic digestion: a review. Renew. Sustain. Energy Rev. 183, 113536.
Zhang, D., Zhang, R., Zheng, Y., Zhang, B., Jiang, Y., An, Z., Bai, J., 2023b. Carbon emission reduction analysis of CHP system driven by biogas based on emission factors. Energy Built Environ. 4 (5), 576–588.
Zhao, X., Chen, H., Li, J., Pan, P., Gui, F., Xu, G., 2024. Thermodynamic and economic analysis of a novel design for combined waste heat recovery of biogas power generation and silicon production. Energy 290, 130272.
Zhou, J., Ali, M.A., Wais, A.M.H., Almojil, S.F., Almohana, A.I., Alali, A.F., Ali, M.R., Sohail, M., 2023. A novel modified biogas-driven electricity/cooling cogeneration system using open-and-closed Brayton cycle concepts: environmental analysis and optimization. Ain Shams Eng. J., 102230